Lasers in Manufacturing Conference 2015

How fast is fast enough in the monitoring and control of laser welding?

Felix Tenner[a,b,*], Florian Klämpfl[a], Michael Schmidt[a,b]

[a]*Institute of Photonic Technologies, Friedrich-Alexander-Universität Erlangen-Nürnberg, Konrad-Zuse-Str. 3/5, 91052 Erlangen, Germany*
[b]*Graduate School in Advanced Optical Technologies, Friedrich-Alexander-Universität Erlangen-Nürnberg, Paul-Gordan-Str. 6, 91052 Erlangen, Germany*

Abstract

In the present study we show how fast the fluid dynamics change when changing the laser power for different feed rates during laser metal welding. By the use of two high-speed cameras and a data acquisition system we conclude how fast we have to image the process to measure the fluid dynamics with a very high certainty. Our experiments show that not all process features which can be measured during laser welding do represent the process behavior similarly well. Despite the good visibility of the vapor plume the monitoring of its movement is less suitable as an input signal for a closed-loop control, due to its high noise. Additionally, the plume does adjust with a delay on a change of process parameters. This physical limit restricts the maximal possible monitoring rate. Therefore, a reliable real-time control of laser welding over a wide range of process parameters might not be possible by the monitoring of the vapor plume. The features measured inside the keyhole show a good correlation with changes of process parameters. Due to its low noise, the area of the keyhole opening is well suited as an input signal for a closed-loop control of the process.

Keywords: Laser welding, monitoring, closed-loop control

1. Introduction

The monitoring and control of laser material processes is in the scope of science and research for almost 30 years. One important requirement of a process control system is the ability to monitor and control the process in real-time. This results in a high demand for monitoring systems with high sample rates. However, closed-loop control systems with control frequencies well above 1 kHz are not generally necessary for the

* Corresponding author. Tel.: +49-9131-85-23236; fax: +49-9131-85-23234.
E-mail address: felix.tenner@fau.de.

control of the laser welding process, since different process features do behave differently with respect to their fluctuations or the delay time after changes of process parameters.

Another important feature of a control system is the reliability. For a desired controlling frequency f_{con} a monitoring frequency f_{mon} is needed. For a reliable monitoring of a process feature f_{mon} has to be well above f_{con} (f_{mon} = X * f_{con}). The value of X depends on the fluctuation of the monitored process feature. For features with small deviations, when using constant process parameters, using only ten measurement values might be enough to assure that the measurement does really represent the process behavior. However, for highly fluctuating features a number of 100 measurement values might be necessary to get a reliable value. For a control frequency of 1 kHz this can easily lead to a sample rate of well above 100 kHz. However, for an industrial application of a control system the costs are very important. These costs do normally increase with the provided sample rate. So, the sample rate should be chosen as low as possible to have reliable control systems.

Summarizing, there is always a need for balancing costs and frame rate of a specific monitoring system. Hence, there is the question: how fast is fast enough? Furthermore, the melt and gas dynamics inside the keyhole might have a certain delay time when changing laser power and feed rate. This delay is a limiting factor for controlling the process. Hence, it has to be known. For a long time it was not possible to measure these small delays. Nowadays, high-speed cameras are capable of imaging these changes in a sufficient time resolution.

2. State of the art

The first approaches for the monitoring of laser material processing have been done over 30 years ago by the use of photodiodes and microphones (Lewis and Dixon, 1985). The monitoring of the process' radiation was thereafter enhanced by evaluating spectral information from the vapor plume (Collur and DebRoy, 1989). These approaches are beneficial for monitoring the highly dynamic laser welding process since a real-time evaluation of the photodiode signals can be done easily. Therefore, photodiode-based measurement systems are available on the market and are still a topic of research (Jurca and Urs, 2010).

Nevertheless, these approaches lag the possibility to have the whole picture of the process and the adjustment of the measurement system is prone to errors, since photodiodes do have a very limited field of view. Furthermore, the process radiation is only an indirect measure of the real process dynamics. A direct camera-based observation of the interaction zone between the laser beam and the material does not suffer from these drawbacks since the whole process and its surrounding is imaged and the sensor system is easily adjustable. With the rise of high-speed cameras in the 1990s first attempts could be made to directly image the interaction zone in laser welding (Voelkel and Mazumder, 1990).

Nevertheless, these approaches have been limited in their significance due to the low magnification which prevents the analysis of fluid dynamics inside the keyhole. Another drawback of this technique is the large amount of data which hampers a real-time processing of the monitoring data. An approach which tackles these issues is the use of cellular neural network cameras which have an image processing unit inside the camera for every single pixel. The use of these cameras enabled a real-time monitoring of the fusion state in laser metal welding (Abt et al., 2011). For the monitoring of process characteristics which do not change rapidly within a couple of milliseconds, like the temperature distribution in the work piece, a real-time monitoring can be realized more easily and thus be better applied in an industrial environment (Friedhelm Dorsch et al., 2012).

However, for an accurate imaging of the fluid dynamic in laser welding, which is the determining factor for seam quality, high spatial and temporal resolution is needed (Eriksson et al., 2013). Since today, no real-time monitoring camera-based device can achieve these resolutions which are in the range between 100 and

300 kHz. Therefore, in the industrial application of process monitoring technique, there is always a trade-off between the processing speed and the accuracy of a specific sensor system. Moreover, the fastest monitoring system cannot control the process in real-time if there are delays in the actuator unit due to mechanical or electronic limitations (e. g. the inertia when increasing the feed rate). Therefore, in most of the cases changing the laser power is used for influencing the process, independent from the monitoring technique. This might be the measurement of the electron temperature (Sibillano et al., 2012), the position of the vapor plume (Brock, 2014) or the measurement of the keyhole depth via white light interferometry (Boley et al., 2014).

Summarizing, there is a lack of real-time control systems which do guarantee a defect-free weld. However, for most of the application scenarios it is not necessary to have a monitoring system which images the welding process in high spatial and temporal resolution, since some process characteristics do not change instantaneously when changing feed rate or laser power. Furthermore, some process characteristics might seem to be measurable quite easily, but they are so inconsistent in their appearance that their measurement might lead easily to errors when using a low frame rate.

3. Experimental setup

To determine how fast a process has to be imaged to measure the fluid dynamics with a high certainty we use two synchronized high-speed cameras (VisionResearch Phantom v1210) working with a frame rate of 240 kHz when using an image size of 128 x 128 pixel (see Fig. 1a)). This setup enables us to conclude what is the maximal useful speed of a control system to have an effect on the fluid dynamics in laser welding. A band-pass filter in front of the cameras prevents reflections of the laser light saturating the images. Since the size of the process features is in the range of some hundred micrometers we use a magnification objective (factor 3) from Navitar to obtain a detailed view at a working distance of approximately 200 mm. For material processing we use a TruDisk 4002 Yb:YAG laser (wavelength 1030 nm, maximum output power 4 kW) coupled to a focusing optic (BEO D70, focal length 200 mm, spot size 600 µm, beam profile top hat).

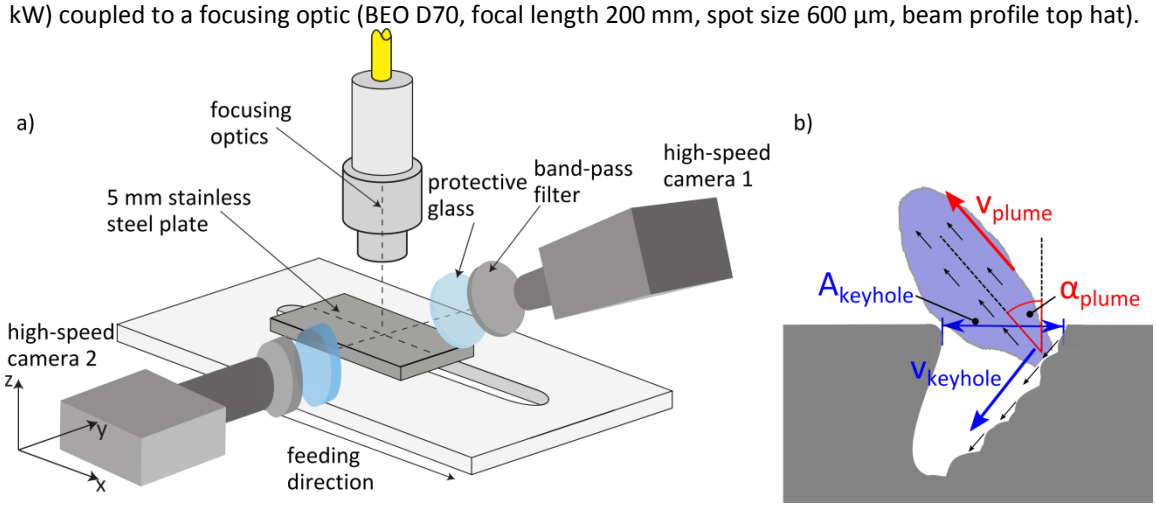

Fig. 1. Setup for measuring the keyhole opening area $A_{keyhole}$, the velocity of the melt at the keyhole front wall $v_{keyhole}$ (both imaged with camera 1), the vapor plume velocity v_{plume} and inclination angle α_{plume} (camera 2), the plume was evaluated in an area with the height of 1.5 mm above the keyhole to avoid influences from the turbulent flows which occur in the top of the plume; camera 1 is inclined by an angle of 55° with respect to the sheet surface; camera 2 is perpendicular to the x-z-plane and inclined by an angle of

We apply this setup to weld into a stainless steel plate (X6CrNiTi18-10) of 5 mm thickness. Due to the thickness of the steel plate we avoid any influences of full penetration of the material. For moving the metal

sheets with high accuracy we use a system of linear stages (Aerotech PRO280LM). Due to the high temporal and spatial resolution of our imaging setup we are able to resolve velocities inside the keyhole of up to

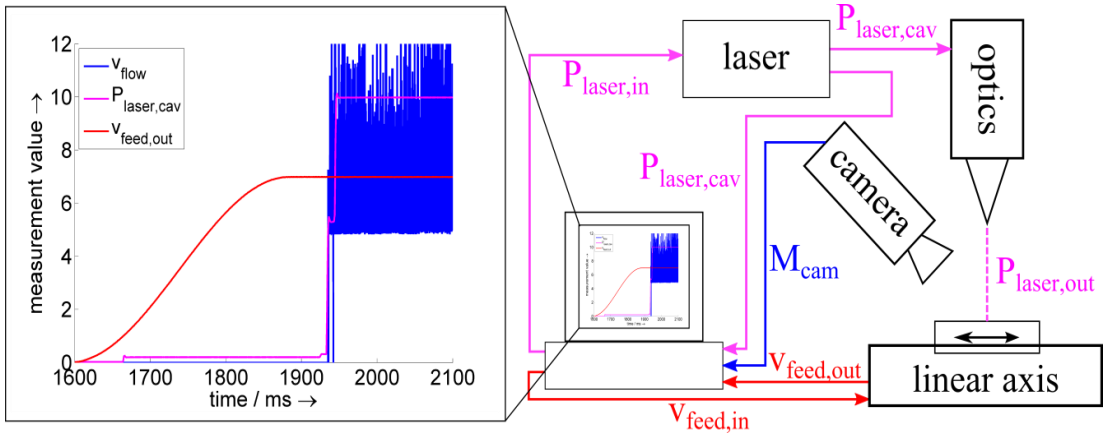

Fig. 2. Data acquisition setup; a specific value for laser power $P_{laser,in}$ and feed rate $v_{feed,in}$ is send from the measurement unit to the laser and the linear axis; during welding the power in the laser cavity $P_{laser,cav}$, the real feed rate $v_{feed,out}$ and the process feature M_{cam} is measured (e.g. the flow at the keyhole front wall v_{flow}); note that $P_{laser,cav}$ is not necessarily equal the laser power at the work piece $P_{laser,out}$ due to losses in the laser optics, these losses are neglected in the present study. The left part of the figure shows an exemplary experiment: The laser power has the unit of W and is divided by a factor of 200 for better comparability with the other values, the flow velocity at the keyhole front has the unit of m/s and the feed rate has the unit of m/min.

several tens of meters per second with certainty, which is necessary for measuring the dynamics of the weld process.

During our experiments we vary laser power and feed rate, since those two parameters are the most widely used parameters to influence the laser welding process in the application of closed-loop control systems. By changing the laser power step-wise for different feed rates the influence on the process behavior can be obtained. The lowest laser power we used was 1500 W. This ensures to have a stable keyhole for all welds and avoids the influence of the transition from heat conduction to deep penetration welding. The feed rate was varied between 2 and 10 m/s. In every experiment we change either the laser power *or* the feed rate to have a better separation of the influences on the process behavior. As measurands we choose process characteristics which are affected by changes of feed rate and laser power. From prior studies we know that the keyhole opening area $A_{keyhole}$ (Abt et al., 2011), the melt flow at the keyhole front wall $v_{keyhole}$ (Eriksson et al., 2010), the vapor plume velocity v_{plume} (Tenner et al., 2014) and the plumes' inclination angle α_{plume} (Fabbro et al., 2006) are affected by the laser power and the feed rate. Hence, these features are in the scope of our present study (as depicted in Fig. 1b)).

For an observation of the keyhole camera 1 was lined up at a 35° angle to the beam axis. Camera 2 was positioned perpendicular to the feeding direction at a 85° angle to look at the vapor plume from its point of formation (the keyhole) to the top. For an undisturbed view at the melt flow inside the keyhole, we used a setup with a glass plate flanking the keyhole as described in detail in (Tenner et al., 2015b).

4. Data evaluation

For a detailed analysis of the process behavior for sudden changes of feed rate and laser power a synchronized evaluation of the process measurement data (keyhole, vapor plume) and the process parameters (feed rate, laser power) is essential. Fig. 2 shows our data acquisition setup. The power in the laser cavity $P_{laser,cav}$ and the feed rate of the linear axis $v_{feed,out}$ are monitored with a frequency of 1 kHz, which

is the maximum available monitoring frequency for the used system. Since the process feature is measured with a frequency of 240 kHz, an interpolation of the monitoring data has to be done. For synchronizing the camera images with the monitoring data we choose the start of every single welding experiment. An increase of laser power from 40 W (stand-by laser power) to 1500 or 2000 W leads to a rapid evolution of melt at the work piece (as shown in Fig. 3). The time from the first visible laser reflection until the evolution of a well visible amount of melt is well below 1 ms. As depicted above, the monitoring frequency of our processing unit, which limits our time resolution, is 1 kHz. Therefore, we can conclude that our method of synchronizing the process images with the monitoring signal by using the first visible laser reflection on the work piece is valid.

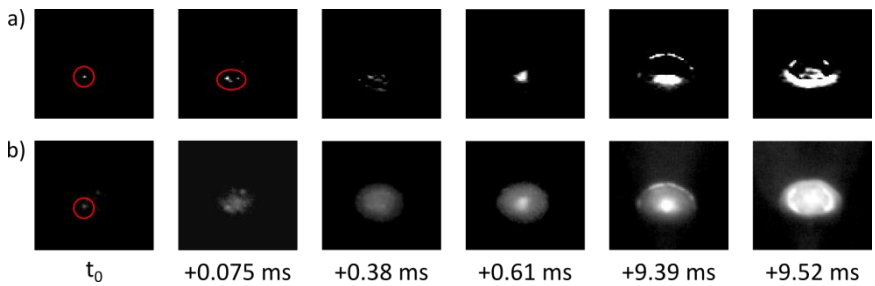

Fig. 3. Processed (a) and original camera image (b) of the keyhole opening at the start of a weld; process status from left to right: first laser reflection on the work piece, steady absorption at the work piece surface, begin of melting, evolution of a melt pool, begin of vaporization, evolution of a keyhole.

The left diagram in Fig. 2 shows an exemplary measurement of the start of a welding experiment. The laser power has the unit of W and is divided by a factor of 200 for better comparability with the other values. The flow velocity at the keyhole front has the unit of m/s and the feed rate has the unit of m/min. As it can be seen, the increase in feed rate does take several hundreds of milliseconds, due to the high inertia of the linear axis. Therefore, we cannot make a statement about the delay time of a process feature for an increase in feed rate in the present study. This issue might only be solved by imaging the process through a laser scanner. However, currently there is no optical system available which allows the process imaging through a laser scanner with the needed spatial and temporal resolution. Nevertheless, we can measure the process behavior for step-wise changes of laser power depending on the used feed rate.

For measuring the process features we use either threshold operations and morphological filters (for the keyhole opening area as shown in Tenner et al., 2015a) or optical flow algorithms (for the vapor plume and the flow inside the keyhole as shown in Tenner et al., 2014).

The number of measuring points needed to calculate a reliable mean value, which is the foundation for a reliable closed-loop control, has a high impact at the maximum reachable controlling frequency. Therefore, the dynamic of a process feature has to be measured.

Commonly, the dynamic range of a system is measured with a frequency analysis. However, the Fourier transformed function of a signal, which is the foundation for a frequency analysis, is a bad representation of the original signal if the periodicity of the original signal is very low. This is the case because low periodicity does normally lead to high frequency components which can exceed the sampling frequency of the signal. Hence, this so-called *aliasing effect* does decrease the significance of a Fourier analysis. To visualize, that the aliasing effect applies to the measurement of process features in laser welding, an example of the temporal course of the inclination of the vapor plume is shown in Fig. 4. There is no periodicity visible in the measurement signal and the oscillation is strongly non-harmonic.

Therefore, for every single laser power / feed rate combination we measure the mean values $\bar{x}_1$ and $\bar{x}_2$ of the process feature and the standard deviation before and after the change in process parameters. For comparing the different features we scale the standard deviation with the specific mean values. This coefficient of variation c_v can then be used as a measure how alternating a process feature is. The higher c_v the more measuring points are needed to calculate a reliable mean value.

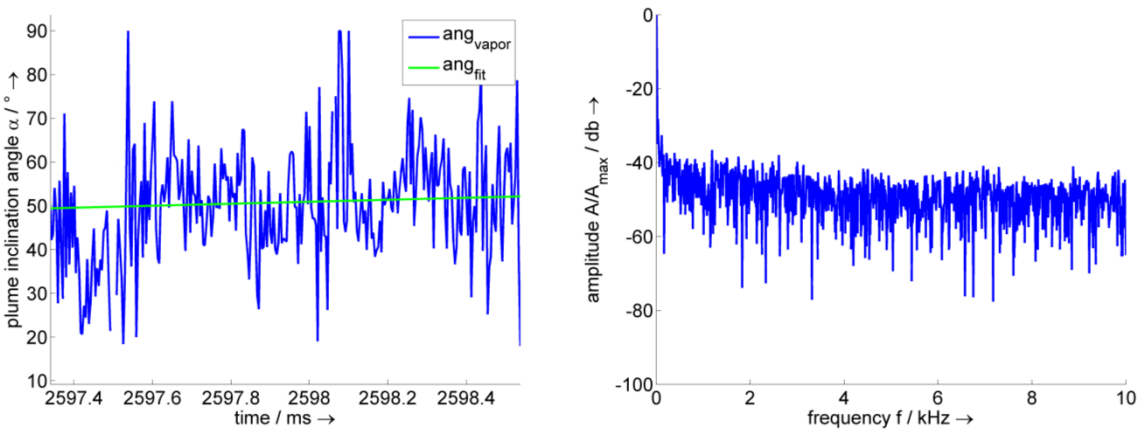

Fig. 4. The left diagram shows an exemplary measurement signal of the vapour plume inclination over time, the fit function represents a mean value of 1000 consecutive data points; the right diagram shoes the FFT of the inclination signal, where no dominant frequency peaks can be obtained.

The differences of the mean values before and after a change in process parameters are a measure for the sensitivity of a process feature. For comparing the differences throughout all process features we normalize the difference with the mean of the two mean values $\bar{x}_1$ and $\bar{x}_2$. An increase of this difference Δ_{norm} gives evidence of an increased controllability of the specific process feature by changing process parameter.

As Fig. 4 shows, the measurement signal is very noisy so the time T_d between a change of a process parameter and the adaption of a process feature cannot be recognized easily. However, from our previous work we know that certain process parameters are correlated with certain process features. Based on this, our assumption is that during a steady process the process features have a constant value. After a change of a process parameter it changes linearly to the new steady value. To get the start and the end of this change we fit such a function onto the measured signal. The steady values are calculated from the measured data by averaging. The start and end point of the linearly increasing or decreasing range are varied until the RMS value between the measured and the modeled signal over a range including also significant periods in steady state reaches a minimum. The result of such a fit can be seen in Fig. 5a).

Fig. 5a) shows the measured process feature as well as the value of our model. When fitting the model, the RMS value is calculated over the whole range where the function is shown. Based on this diagram, it cannot be judged how well the fit models the data and how unique the fit is. To answer this, Fig. 5b) shows the RMS value for different start and end points of the linearly changing range of the fit function. The investigated range has been chosen manually from Fig. 5a), but as Fig. 5a) shows, it is valid to assume that the change of the flow velocity of the plume happens somewhere during this time.

It can be clearly seen that the RMS value has a minimum (white dot in Fig. 5b)) at a starting time of approx. 2356 ms and an end time of approx. 2365 ms. This is apparently a global minimum and no other starting and end times might be a candidate for another minimum. Therefore, it can be concluded that the

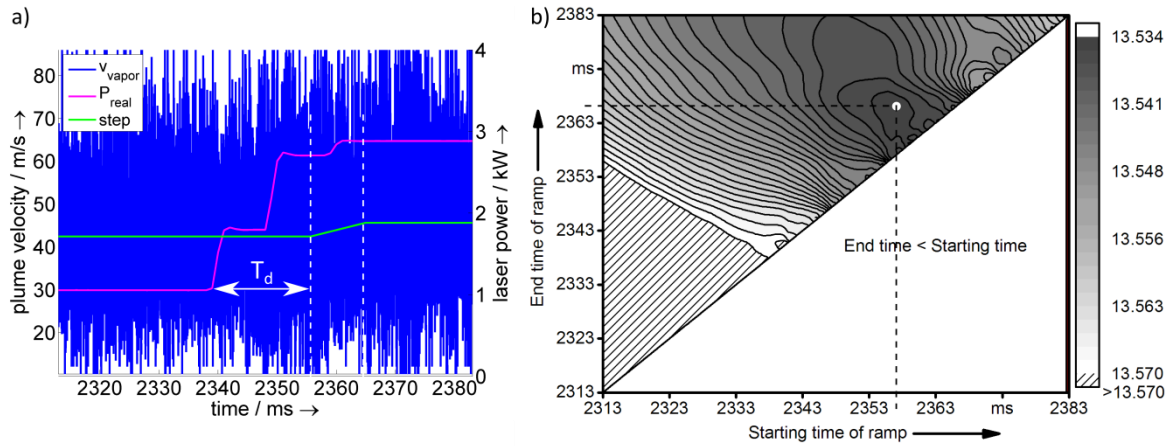

Fig. 5 The left diagram shows an exemplary measurement of the plume flow velocity during an increase of laser power with the measured delay time T_d; the right diagram shows a contour plot of the RMS value calculated between measured values and fit function depending on the starting and end time of the linearly changing range of the fit function

chosen fitting approach works well. The corresponding fit is shown in Fig. 5a) in green. Furthermore, the measured delay time T_d can be obtained.

5. Results

The results of the measurement of the keyhole opening $A_{keyhole}$, the flow velocity at the keyhole front wall $v_{keyhole}$, the inclination angle α_{plume} and the velocity of the vapor plume v_{plume} are shown in Fig. 6.

Fig. 6a) and b) show the coefficient of variation c_v for a constant laser power of 1.5, 2.25 and 3.25 kW and a feed rate of 4 and 7 m/min. c_v shows no clear trend in dependence of the laser power. However, a slight decrease of c_v can be seen for a higher feed rate. This trend can also be seen for a feed rate of 2 m/min (large c_v) and 10 m/min (small c_v). When comparing the c_v of the specific process features it can be obtained that the vapor plume has a higher dynamic than the keyhole opening or the melt flow at the keyhole front. Consequently, the high dynamic of the plume movement demands a high temporal resolution of the measurement system. Hence, using the vapor plume movement as an input signal for a closed-loop control is linked to a higher monitoring frequency for measuring a reliable mean value.

Fig. 6c) and d) show the normalized difference Δ_{norm} for an increase of the laser power ΔP by 0.75, 1.25 and 1.75 kW. As expected, a higher increase of laser power leads to a larger Δ_{norm}. It is clearly visible that the keyhole opening area is the most sensitive feature for an increase of laser power. Hence, this features does well represent the current process state and is therefore ideal for the use in a closed-loop control. Furthermore, the opening area is the only feature in our study which fluctuations for constant process parameters are smaller than the deviations when changing the process parameters. Therefore, only one image of the opening area can be a significant measure of the current process behavior.

Fig. 6e) and f) show the delay time T_d. Unlike in the graphs before, where the values where equal for the case of increasing and decreasing laser power, the delay time is depending on the gradient of the laser power change. Since T_d was below 1 ms for $A_{keyhole}$ and $v_{keyhole}$ only the process features of the vapor plume are shown. The small T_d of the keyhole features confirms our assumption that a change of process parameters does affect the keyhole related process features instantaneously. Whereas, the plume features show a change of Δ_{norm} only after a specific time delay. The movement of the plume is delayed by up to 35 ms. This physical limit restricts the maximal possible monitoring rate to approx. 28 Hz. The inclination angle

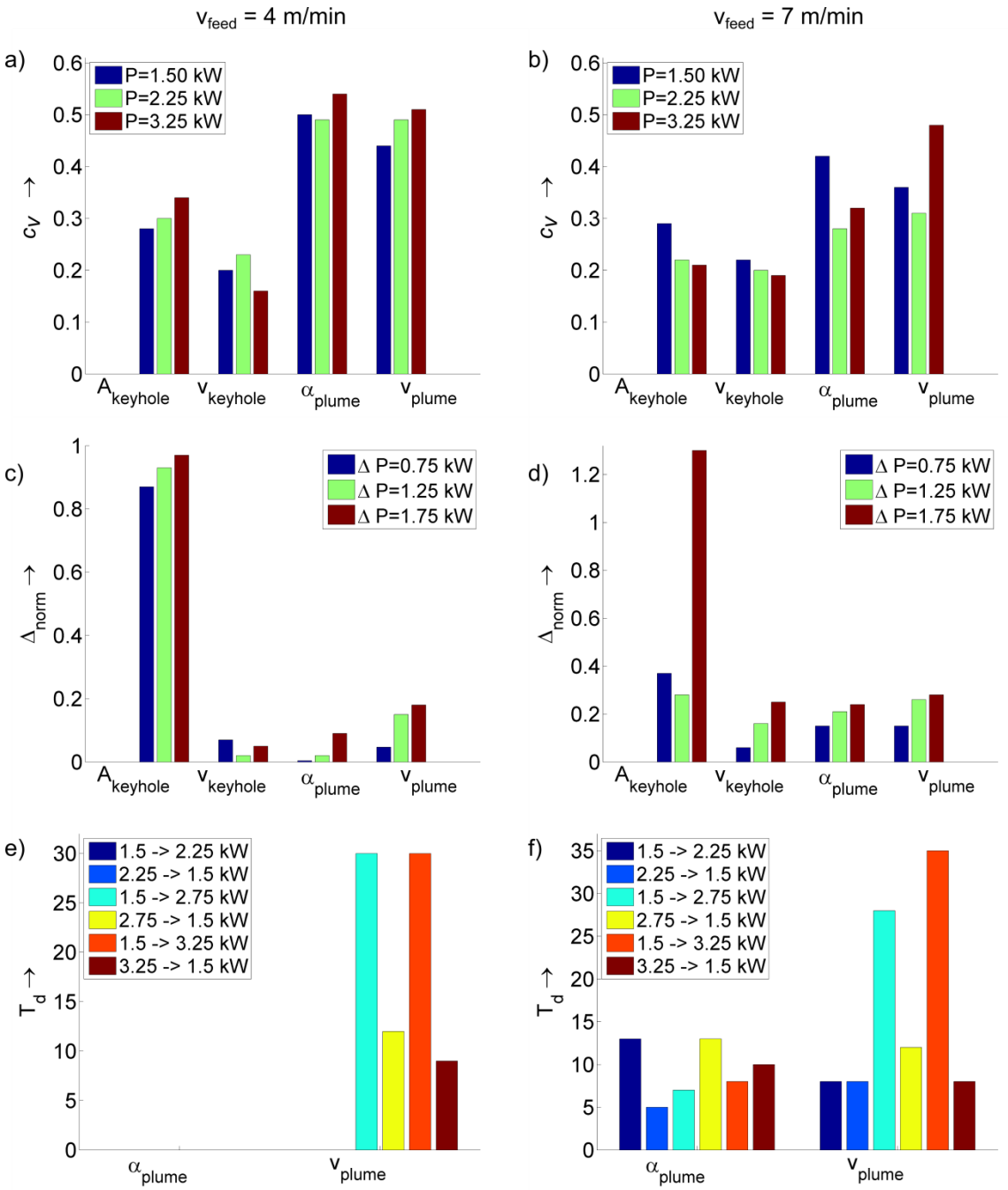

Fig. 6. Final results of our measurements of the keyhole opening $A_{keyhole}$, the flow velocity at the keyhole front wall $v_{keyhole}$, the inclination angle α_{plume} and the velocity v_{plume} of the vapour plume: a) and b) show the coefficient of variation c_v for a constant laser power and feed rate of 4 and 7 m/min; c) and d) show the normalized difference Δ_{norm} for an increase of laser power for the two different feed rates 4 and 7 m/min; e) and f) show the delay time T_d for rising and falling laser power steps, note that the values for $A_{keyhole}$ and $v_{keyhole}$ are not shown due to the fact that the delay time was below 1 ms in the measurements.

of the plume shows a shorter delay, but the measured values in the range of 15 ms do still limit the monitoring rate to 66 Hz. The absence of a delay for the keyhole features shows that the process dynamics change in the order of well above 1 kHz.

For explaining the measured behavior the driving factors of the fluid dynamics inside the keyhole have to be considered. The downward directed melt flow waves at the keyhole front wall are induced by the evaporation due to the absorbed laser beam energy (Kaplan, 2012). Due to the fact that the laser power is approximately constant over time and over the area of the keyhole front wall (because of the top-hat profile of the laser beam) a constant melt flow without fluctuations is evolving. In contrast, the vapor plume is strongly fluctuating for constant process parameters. This has two major reasons: On the one hand, the prementioned wavy keyhole front leads to a fluctuating evaporation direction throughout the keyhole front wall. On the other hand, the vapor plume does randomly interact with the melt pool behind the keyhole. If the plume hits the melt pool the vapor velocity is decreasing for a moment and increases afterwards quite rapidly which leads to a highly dynamic behavior.

However, the higher the feed rate the lower the dynamic of the plume. This can be explained by the observation of a faster melt flow inside the keyhole for higher feed rates (Tenner et al., 2015b). An increase in melt flow velocity is caused by an increase in evaporation pressure, since this pressure is the driving force of the melt flow. The evaporation pressure is counteracting with the hydrostatic pressure of the melt pool. The stronger the evaporation pressure the smaller is the influence of the melt pool dynamics. Hence, a more directed evaporation leads to a lower fluctuation of the vapor plume. This behavior can also be seen by the decrease of c_v of $A_{keyhole}$ for an increase in feed rate, since $A_{keyhole}$ is also determined by the equilibrium between the evaporation pressure and the hydrostatic pressure of the melt pool. The fact that Δ_{norm} is the highest for $A_{keyhole}$ can also be explained by the influencing factors of the keyhole opening area. The increase of the mass of evaporated material and hence the increase in flow velocity inside the keyhole and the vapor plume do both contribute to an increasing keyhole opening area. Therefore, their increase does lead to a multiplied increase of the keyhole opening area. However, all features show an increase of Δ_{norm} when increasing the feed rate, which is an outcome of the prementioned increase of fluid dynamics with increasing feed rate.

For explaining the time delay of the plume velocity the evaporation process has to be considered on a microscopic and a macroscopic scale. As the melt waves at the keyhole front (which have a neglible T_d) are generated by evaporation it has to be assumed that the evaporation does increase instantaneously for an increase of laser power. So, there is no significant delay when we look at the microscopic scale of the evaporation (e. g. the Knudsen layer). Therefore, the T_d of the plume's velocity and inclination angle has been generated due to the rapidly changing and non-uniformly evolving evaporation behavior at the keyhole front. This can lead to a delayed change of the velocity and the direction of the vapor plume in a macroscopic scale (e. g. the part of the plume we can image with a monitoring system). The smaller T_d for a decrease of laser power is caused by the sudden collapse of evaporation which cuts the source of the vapor flow. Therefore, the described delay is not as high for a decrease of laser power compared to an increase.

6. Conclusion and outlook

Our experiments show that not all process features which can be measured during laser welding do represent the process behavior at the same level. Despite the good visibility of the vapor plume the monitoring of its movement is less suitable as an input signal for a closed-loop control, compared to features inside the keyhole, because the high dynamic of the plume movement demands a high temporal resolution of the measurement system. Additionally, the movement of the plume shows a delay with respect to changing process parameters. Therefore, a reliable real-time control of laser welding over a wide range of

process parameters might not be possible by the monitoring of the vapor plume. However, there might be process windows where a low control frequency in the range of 20 Hz is sufficient to control the process with high reliability.

The features inside the keyhole show a good correlation with a change of process parameters. Especially the keyhole opening is well suited as an input signal for a closed-loop control of the process, since the fluctuations for constant process parameters are smaller than the deviations when changing the process parameters. This leads to a theoretically possible control frequency in the order of the monitoring frequency and the value X (f_{mon} = X * f_{con}) can be one. However, in a real application a value X of five to ten might be advisable for a reliable closed-loop control.

In future work, we want to use the knowledge we gained in the present analysis to build sensor and control systems for industrial application and to compare our findings with simulation models.

Acknowledgements

The authors gratefully acknowledge funding of the German Federal Ministry of Education and Research by the funding program Photonics Research Germany (contract number 13N12134) and funding of the Erlangen Graduate School in Advanced Optical Technologies (SAOT) by the German Research Foundation (DFG) in the framework of the German excellence initiative.

References

Abt, F., Heider, A., Weber, R., Graf, T., Blug, A., Carl, D., Höfler, H., Nicolosi, L., Tetzlaff, R., 2011. Camera Based Closed Loop Control for Partial Penetration Welding of Overlap Joints. Physics Procedia 12, 730–738.

Boley, M., Webster, P., Heider, A., Weber, R., Graf, T., 2014. Investigating the Keyhole Behavior by Using X-Ray and Optical Depth Measurement Techniques. In: , Proceedings of the ICALEO 2014. Laser Institute of America, pp. 426–430.

Brock, C., 2014. Analyse und Regelung des Laserstrahltiefschweißprozesses durch Detektion der Metalldampffackelposition. Meisenbach, Bamberg, VI, 116 S.

Collur, M.M., DebRoy, T., 1989. Emission spectroscopy of plasma during laser welding of AISI 201 stainless steel. Metallurgical and Materials Transactions B 20, 277–286.

Eriksson, I., Gren, P., Powell, J., Kaplan, A.F.H., 2010. New high-speed photography technique for observation of fluid flow in laser welding. Opt. Eng. 49 (10), 100503.

Eriksson, I., Powell, J., Kaplan, A.F.H., 2013. Melt behavior on the keyhole front during high speed laser welding. Optics and Lasers in Engineering 51, 735–740.

Fabbro, R., Slimani, S., Doudet, I., Coste, F., Briand, F., 2006. Experimental study of the dynamical coupling between the induced vapour plume and the melt pool for Nd–Yag CW laser welding. J. Phys. D: Appl. Phys. 39, 394–400.

Friedhelm Dorsch, F., Braun, H., Keßler, S., Pfitzner, D., Rominger, V., 2012. Detection of faults in laser beam welds by near-infrared camera observation. International Congress on Applications of Lasers and Electro Optics (ICALEO), pp. 212–219.

Jurca, M., Urs, C., 2010. Novel noncontact temperature fiber sensor for multi-spot field measurements. 2010 International Symposium on Optomechatronic Technologies, ISOT 2010.

Kaplan, A.F.H., 2012. Fresnel absorption of 1µm- and 10µm-laser beams at the keyhole wall during laser beam welding: Comparison between smooth and wavy surfaces. Applied Surface Science 258, 3354–3363.

Lewis, G.K., Dixon, R.D., 1985. Plasma monitoring of laser beam welds. Welding Journal 64, 49–54.

Sibillano, T., Rizzi, D., Mezzapesa, F.P., Lugarà, P.M., Konuk, A.R., Aarts, R., Veld, Bert Huis In 't, Ancona, A., 2012. Closed loop control of penetration depth during CO_2 laser lap welding processes. Sensors (Basel, Switzerland) 12, 11077–11090.

Tenner, F., Brock, C., Gürtler, F.-J., Klämpfl, F., Schmidt, M., 2014. Experimental and Numerical Analysis of Gas Dynamics in the Keyhole During Laser Metal Welding. Physics Procedia 56, 1268–1276.

Tenner, F., Brock, C., Klämpfl, F., Schmidt, M., 2015a. Analysis of the correlation between plasma plume and keyhole behavior in laser metal welding for the modeling of the keyhole geometry. Optics and Lasers in Engineering 64, 32–41.

Tenner, F., Berg, B., Brock, C., Klämpfl, F., Schmidt, M., 2015b. Experimental approach for quantification of fluid dynamics in laser metal welding. J. Laser Appl. 27, S29003.

Voelkel, D.D., Mazumder, J., 1990. Visualization of a laser melt pool. Appl. Opt. 29, 1718–1720.